Magneto-Electric Diffusion of Electrons in Gallium Nitride: a Monte Carlo Analysis

G. I. Syngayivska*, V. Korotyeyev*, V. A. Kochelap*, L. Varani†
*V. Lashkaryov Institute of Semiconductor Physics,
NAS of Ukraine, 41 prospect Nauky, 03680 Kyiv, Ukraine
†Institute of Electronics and Systems (CNRS UMR 5214),
University of Montpellier, 860 rue St. Priest, 34095 Montpellier, France

***Abstract*—We present a Monte Carlo analysis of the diffusion coefficient tensor in compensated bulk Gallium Nitride for parallel and crossed configurations of the electric and magnetic fields. We found that at low lattice temperatures and low impurity concentrations, the electric-field dependences of the transverse–to–current components of the diffusion tensor are non-monotonic for both configurations, while the diffusion processes are mainly controlled by the magnetic field. With increasing the lattice temperature or impurity concentration, the behaviour of the diffusion tensor becomes more monotonic and less affected by the magnetic field. We showed that this behaviour is caused by the peculiar kinetics of hot electrons in polar semiconductors with strong electron–optical phonon coupling.**

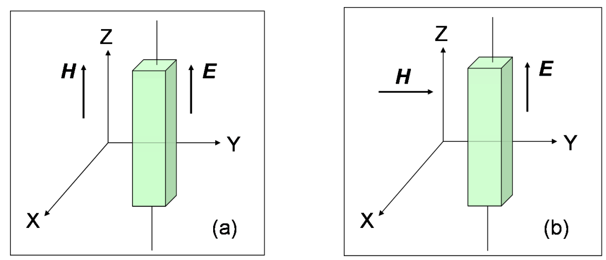

Fig. 1. Scheme of parallel (a) and crossed (b) configurations of E and H.

I. Introduction

The nitride compounds represent nowadays perspective materials for many practical applications like light-emitting diodes [1], optical switches [2], biosensors [3] and terahertz devices such as electrically pumped terahertz sources [4], detectors [5] and modulators [6]. For these reasons a lot of attention has been recently devoted to the investigation of their electron transport properties not only in the presence of electric but also magnetic fields in order to develop novel devices working as sensors and switches controlled by a magnetic field [7]–[9]. Furthermore, nitrides are also favorable materials for the realisation of a remarkable electron transport regime characterised by a quasi-periodic electron motion in the momentum space due to the strong threshold character of the electron–optical phonon emission [10]. This so-called *streaming* regime may produce plenty of interesting phenomena among which we can mention the saturation of the current-voltage characteristics, the appearance of a negative dynamic conductivity and a strong non-monotonic behaviour of the diffusion coefficient. Additional useful information about the *streaming* regime can be obtained investigating the galvanomagnetic characteristics at different configurations of the electric and magnetic fields. In particular, we have recently shown that, in compensated Gallium Nitride, the electron transport may take the form of a vortex-like motion in momentum space and the magnetic field may induce a collapse of the dissipative current due to the suppression of optical–phonon emission [11]. The present interest in the study of the diffusion processes is also inspired by the development of recent pure all-optical pump-probe techniques known as light-induced transient grating, allowing the experimental determination of the diffusion coefficient as well as the carrier recombination times [12].

In this dynamic scientific context it is noteworthy to present a study by Monte Carlo simulations of the diffusion properties of hot electrons in compensated bulk-like GaN samples for various lattice temperatures and impurity concentrations in the presence of parallel and crossed electric and magnetic fields.

II. Theoretical Model

We consider the electron transport in samples of cubic GaN under parallel and crossed configurations of electric, E, and magnetic, H, fields. At $E \parallel H$, we assume that E and H are directed along the z-axis (see Fig. 1 (a)).In the case $E \perp H$, we assume that E and H are applied along the z- and y-axis, respectively (see Fig. 1 (b)). Here, the GaN-samples are assumed to be with short-circuited Hall contacts. To calculate electron transport characteristics, we used the single-particle algorithm of the Monte Carlo procedure [11]. Three main scattering mechanisms were taken into account: electron scattering by ionized impurities, acoustic phonons and polar optical phonons. We considered a range of electric fields for which the intervalley transitions to the upper valleys are absent and the electron dispersion law can be considered as parabolic. The electron-electron scattering was not included into these calculations, because only small electron concentrations were considered. The components of the diffusion tensor D_{ij} are calculated by means of the correlation functions according to the following equation :

$$D_{ij} = \frac{1}{2}\frac{d}{dt}\langle (r_i(t) - \langle r\rangle)\,(r_j(t) - \langle r\rangle)\rangle \qquad (1)$$

where $r_{i,j}$ are the simulated values of the three electron coordinates as functions of time which include random collisions (i.e. diffusion noise) associated with scattering processes and the angle brackets denote the time average.

III. Transport properties without magnetic field

We present the transport properties for three particular examples, which differ by the lattice temperature T_0, the concentration of ionized impurities N_i and the electron concentration N_e. For the case I we assume $N_i = 10^{16}$ cm^3, $N_e = 10^{15}$ cm^3 and $T_0 = 30$ K, for the case II we assume $N_i = 10^{17}$ cm^3, $N_e = 10^{16}$ cm^3 and $T_0 = 30$ K, and for the case III we assume $N_i = 10^{16}$ cm^3, $N_e = 10^{15}$ cm^3 and $T_0 = 300$ K. The results of calculation are shown in Fig. 2. As expected, the characteristic features of the streaming

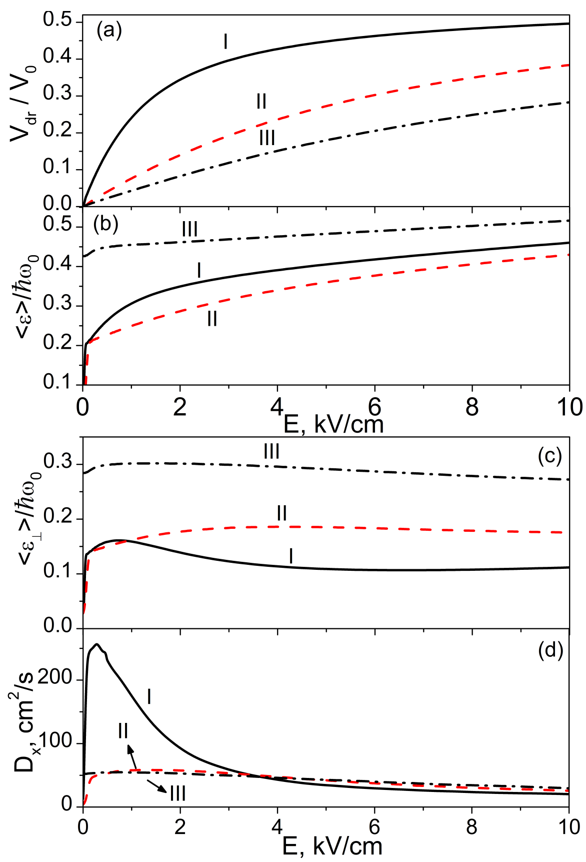

Fig. 2. Drift velocity (a), average electron energy (b), transverse component of the average energy (c) and diffusion coefficient (d) as functions of E at $H = 0$ for three cases (curves I, II, III) discussed in the text. $V_0 = 4 \times 10^7$ cm/s and $\hbar\omega_0 \simeq 92$ meV.

regime are observed only for the sample I. In the range of $E = 3$–10 kV/cm, the drift velocity and the average energy saturate (see Figs. 2(a) and (b)) reaching one half of the characteristic velocity $V_0 = \sqrt{2\hbar\omega_0/m^*}$ and about one third of the characteristic energy $\hbar\omega_0$, respectively. In contrast, for the case II with larger impurity concentration, a well-developed streaming regime is not formed. At room temperature, in the range of $E = 3$–10 kV/cm, the electron gas remains almost at equilibrium, so $V_d(E)$ shows a linear behaviour and $\langle\varepsilon\rangle(E)$ is close to its equilibrium value of $3k_BT_0/2$. The emergence of the streaming regime can be clearly identified by the strong non-monotonic field dependence of the transverse component of the average electron energy $\langle\varepsilon_\perp\rangle$ for the case I (see Fig. 2(c)). The increase at E up to about 1 kV/cm is associated with heating of the electron gas, while with further increasing the field, $\langle\varepsilon_\perp\rangle$ decreases due to the formation of a streaming-like distribution function elongated along the field direction [13]. This decrease tends to saturate in the field range 3–10 kV/cm. For the cases II and III, the streaming is not formed, and $\langle\varepsilon_\perp\rangle$ exhibits only a slightly non-monotonic behaviour.

The field dependency of the transverse component of the diffusion coefficient $D_{xx}(E)$ (shown in Fig. 2(d)) are qualitatively similar to that of $\langle\varepsilon\rangle$ and is associated with the streaming regime that is realized for the case I. At $E < 0.5$ kV/cm, the magnitude of $D_{xx}(E)$ rapidly increases from the equilibrium value of 13 cm^2/s to a maximum of about 250 cm^2/s dut to the electrons isotropic spreading in the transverse direction. The maximum of $D_{xx}(E)$ corresponds to the electric field at which the rapid spreading of the distribution function is terminated and a significant part of high-energy electrons loses its energy due to emission of optical phonons. At further increasing E, the streaming-like distribution function begins to form and D_{xx} rapidly decreases approaching 20–25 cm^2/s at $E > 5$ kV/cm. For the cases II and III, $D_{xx}(E)$ slowly decreases from 50 down to 30 cm^2/s with increasing E from 1 up to 10 kV/cm.

IV. Diffusion coefficient for $E \parallel H$

It should be noted that for electrons with parabolic dispersion law, the application of a magnetic field along the direction of the electric field has no effect on $V_d(E)$ and $\langle\varepsilon_\perp\rangle(E)$ because the electron motions in the directions along and transverse to the fields are uncoupled [14] However, the electron diffusion process shows a strong dependence on the magnetic field. Fig. 3 presents the electric field dependences of the transverse component $D_{xx}(E)$, calculated for three values of H where panels (a), (b) and (c) correspond to the cases I, II and III, respectively. For comparison, $D_{xx}(E)$ at $H = 0$ is shown by the dashed curve while the curves 1, 2 and 3 correspond to three magnitudes of the magnetic field: 1.1, 2.3 and 3.4 T, respectively. The behaviour of $D_{xx}(E)$ in magnetic field has the following general peculiarities for all the cases: (i) the dependences are non-monotonic with their maximum shifted to the higher electric fields with increasing H; (ii) the magnetic field suppresses diffusion in transverse directions with respect to E and H; (iii) the effect of magnetic field decreases at higher electric fields. The magnetic field effect on the electron diffusion is more important for the case I, for which the streaming regime is realized. Even at weak magnetic fields, we observe a strong suppression of the maximum diffusion coefficient, which decreases from ≈ 250 cm^2/s at $H = 0$ down to ≈ 60 cm^2/s at $H = 1.1$ T. With further increasing the magnetic field, the maximum D_{xx} progressively decreases down to 30 cm^2/s at $H = 2.3$ T and approximately

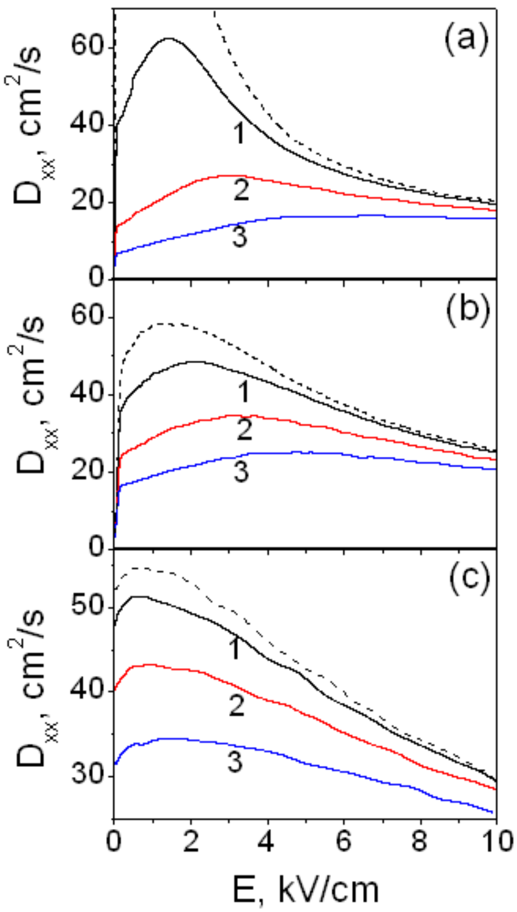

Fig. 3. Dependences of $D_{xx}(E)$ at $E \parallel H$ for the case I (a); II (b); III (c) at $H = 0$ (dashed curves), $H = 1.1$ T (curves 1), 2.3 T (curves 2), 3.4 T (curves 3).

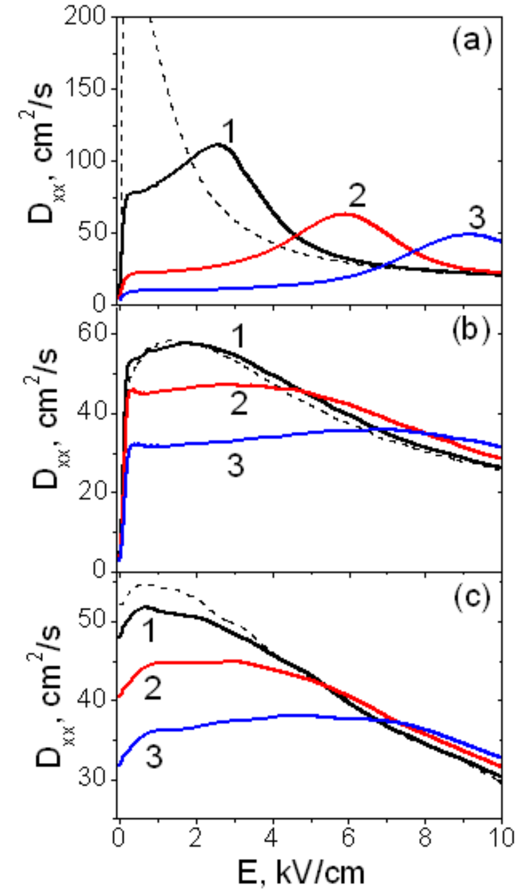

Fig. 4. Dependences of $D_{xx}(E)$ at $E \perp H$ for the case I (a); II (b); III (c) at $H = 0$ (dashed curves), $H = 1.1$ T (curves 1), 2.3 T (curves 2), 3.4 T (curves 3).

15 cm^2/s at $H = 3.4$ T. The position of the maximum diffusion coefficient corresponds to electric fields of 0.5, 1.5, 3 and 5.5 kV/cm for $H = 0$, 1.1, 2.3 and 3.4 T, respectively.

For the cases II and III, for which the streaming regime does not occur, the magnetic field weakly modifies the diffusion coefficient. For example, the maximum D_{xx} decreases only twice from $\simeq 60$ cm^2/s at $H = 0$ down to $\simeq 30$ cm^2/s at $H = 3.4$ T.

Summarizing: the results of the modelling of diffusion processes in compensated GaN show that the largest variations of D_{xx} with the magnetic field occur in the samples for which the streaming electron transport is formed.

V. Diffusion coefficient for $E \perp H$

In this section, we consider the field dependences of the components of the diffusion tensor corresponding to the transverse motion with respect to the electric field direction (see Fig. 1(b)): the D_{xx} component describes the diffusion current perpendicular to E and H while the D_{yy} component characterises the diffusion in the direction parallel to H and perpendicular to E. As previously discussed [11], [15], [16], the magnetic field for this configuration strongly affects the transport characteristics. In particular, the streaming transport regime can be destroyed by the magnetic field, forming a vortex-like distribution function in the momentum space. The result of the measurements of current-voltage characteristics depends on the form of the external circuits. Our transport model assumes the short-circuited Hall contacts. The behaviour of D_{xx} has the same features (i)-(iii) listed in previous section. Indeed, as seen from Fig. 4(a), the impact of the magnetic field on the diffusion is largest for the case I. The dependences of D_{xx} show non-monotonic behavior with a maximum shifted to the region of higher electric fields with increasing H. However there is also a region of electric fields where the diffusion is higher than at $H = 0$. This peculiarity was absent in the case of $E \parallel H$. Moreover, the shift of the maximum D_{xx} is more evident for the configuration $E \perp H$. For the cases II and III (panels (b) and (c) in Fig. 4, respectively), the effect of the magnetic field is weak, the dependences of D_{xx} are weakly non-monotonic with an extended region of electric fields $E = 1$–6 kV/cm (at $H = 2.3$–3.4 T) where D_{xx} is practically constant.

In contrast to the parallel configuration of E and H, in the crossed configuration D_{xx} and D_{yy} are not equal. The electric field dependences of D_{yy} at several values of H are shown in Fig. 5. In general, the increase of H leads to a growth of electron diffusion in the y-direction for a wide range of electric fields. In particular, for the case I (see panel (a) in Fig. 5) the amplitude and position of the maximum are weakly modified with increasing H within the range 1.1–3.4 T. However, at weak magnetic fields, 0–1.1 T, the maximum D_{yy} is twice increased. With increasing electric field, diffusion along the direction of magnetic field progressively decreases, and at $E >$ 6 kV/cm it tends to the case corresponding to $H = 0$. For the case II, the impact of magnetic field on D_{yy} is not so evident as for the case I: its maximum is increased by $\simeq 30\%$ with increasing the magnetic field from 0 up to 3.4 T. For the case III, the magnetic field does not have any influence on D_{yy}.

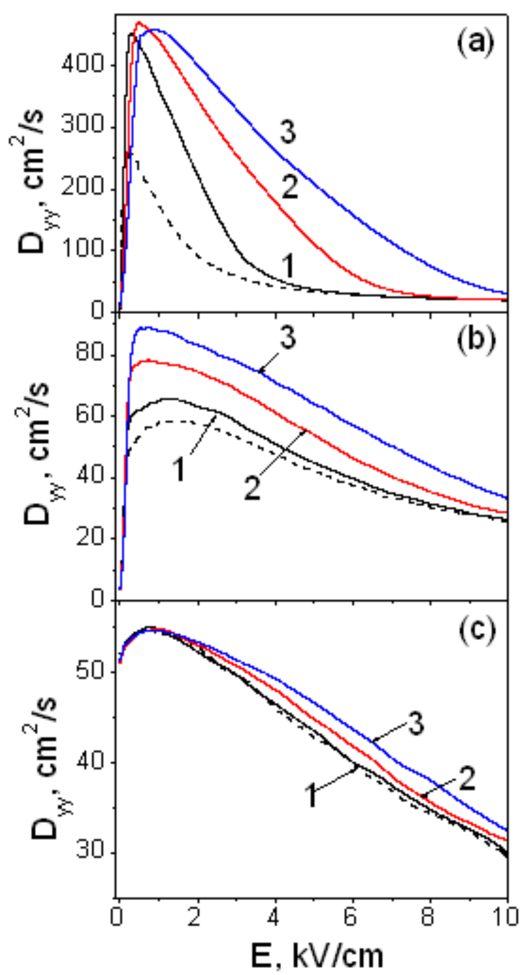

Fig. 5. Dependences $D_{yy}(E)$ at $E \perp H$ for the case I (a); II (b); III (c) at $H = 0$ (dashed curves), $H = 1.1$ T (curves1), 2.3 T (curves 2), 3.4 T (curves 3).

VI. Conclusions

We have presented a Monte Carlo analysis of the diffusion coefficient in Gallium Nitride as a function of electric and magnetic fields in parallel and perpendicular configurations. Three samples have been considered: sample I with low concentration and low temperature, sample II with high concentration and low temperature and sample III with low concentration and room temperature. We have found that the strongest impact of magnetic field on the diffusion properties of the electron gas takes place for the sample I. In the parallel configuration of E and H, the electric field dependences of the transverse-to-current components of the diffusion tensor exhibit a non-monotonic behaviour with a maximum whose amplitude and position depend on the magnitudes of magnetic field. In particular, the maximum decreases and its position is shifted to higher electric fields at increasing values of the magnetic field. In the crossed configuration of E and H, the transverse-to-fields component of the diffusion tensor has similar behaviour. However, the positions of the maximum are more sensitive to the variation of H. The suppression of electron diffusion in the transverse–to–H direction with the increase of magnetic field is a general phenomenon that is observed in both configurations. However, in the crossed configuration, the magnetic field enhances electron diffusion along the H direction. The electric field dependences of the longitudinal-to-H component of the diffusion tensor also have the maximum but both position and amplitude of the maximum weakly depend on the values of H. The physical parameters of the samples II and III prevent the formation of the streaming transport regime and this is the main reason of the weak influence of electric and magnetic fields on diffusion properties in these samples. However, the main peculiarities observed in the field dependences of diffusion processes for the sample I take place for the samples II and III as well. We suggest that the streaming transport regime and related magneto-transport effects can be investigated by measurements of the diffusion effects of hot electrons in electric and magnetic fields using, for instance, electro-gradient and optical measurements of the diffusion coefficient. Finally we emphasise that the knowledge of the far–from–equilibrium dependences of the diffusion coefficient is important for the modelling of electronic devices operating in strong electric and magnetic fields.

References

[1] Lu N. and I. Ferguson, Semicond. Sci. Technol. **28**, 074023 (2013)
[2] M. Beeler et al., Semicond. Sci. Technol. 2013. **28**, 074022 (2013)
[3] V. A. Sydoruk et al., Nanotechnology **28**, 135204 (2017).
[4] K. Ahi, Opt. Eng. **56** 090901 (2017)
[5] W. Knap W et al., J. Appl. Phys. **91**, 9346 (2002)
[6] T. Laurent et al., Appl. Phys. Lett. **99**, 082101 (2011)
[7] G. Santoruvo et al., Appl. Phys. Lett. **109**, 103102 (2016)
[8] L. Bouguen et al., Appl. Phys. Lett. **92**, 043504 (2008)
[9] A. M. Gilbertson et al., Appl. Phys. Lett. 2011. **98**, 062106 (2011)
[10] E. Starikov et al., Phys. Rev. B. **76**, 045333 (2007)
[11] G. I. Syngayivska et al., J. Appl. Phys. **120**, 095704 (2016)
[12] R. Aleksiejunas et al., Sci. Reports. **8**, 4621 (2018)
[13] G. I. Syngayivska and V. V. Korotyeyev, Ukr. J. Phys. **58**(1), 40 (2013)
[14] G. I. Syngayivska et al., Semicond. Sci. Technol. textbf28(3), 035007 (2013)
[15] I. I. Vosilius I.I. and I. B. Levinson, Soviet Physics JETP **25**(4), 672 (1967)
[16] V. A. Kochelap et al., J. Phys. Conf. Series **647**, 012050 (2015)